

We are IntechOpen, the world's leading publisher of Open Access books Built by scientists, for scientists

6,900

Open access books available

186,000

International authors and editors

200M

Downloads

Our authors are among the

154

Countries delivered to

TOP 1%

most cited scientists

12.2%

Contributors from top 500 universities



WEB OF SCIENCE™

Selection of our books indexed in the Book Citation Index
in Web of Science™ Core Collection (BKCI)

Interested in publishing with us?
Contact book.department@intechopen.com

Numbers displayed above are based on latest data collected.
For more information visit www.intechopen.com



Ga³⁺ Focused Ion Beam for Piezo Electric Nano Structuration Fabrication

D. Rémiens¹, D. Deresmes², D. Troadec² and J. Costecalde¹

¹*Institut d'Electronique de Microélectronique et Nanotechnologies (IEMN)*

²*Université de Valenciennes et du Hainaut Cambrésis (UVHC)*
France

1. Introduction

Piezoelectric nanostructures are currently of the potential interest for the development of MEMS / NEMS (Micro / Nano-Electro-Mechanical Systems). Their main applications in the biomedical domains (micro / nano bio actuators and sensors), in automobile industry (actuators and sensors) and in aeronautic industry (health control monitoring) are based on $\text{PbZr}_{0.54}\text{Ti}_{0.46}\text{O}_3$ (PZT) recognized as leading material for these piezoelectric micro/nano devices.^{1, 2, 3, 4} The fabrication of piezoelectric nanostructures on pure PZT (or “doped- PZT”) films is frequently performed by means of Reactive Ion Etching (RIE or ICP (Inductively Coupled Plasma) –RIE with fluorine and/or chlorine gases), Reactive Ion Beam Etching (RIBE), Focused Ion Beam (FIB) Ga³⁺ etching and electron beam direct writing.^{5, 6, 7, 8} In the present study we focus our results on Ga³⁺ FIB etching of PZT nano structures. Typically, the obtained results show that it is possible to fabricate nanostructures with very small lateral size (50 nm on PZT films) when the films are etching in amorphous state followed by a post annealing treatment at the temperature which correspond to the perovskite formation temperature; the piezoelectric properties are similar to those obtained on un etched PZT films. Any degradation is observed. For crystallized films, the situation is completely different: no ferroelectric properties are observed after etching and the piezoelectric-response is strongly degraded. A post annealing treatment in oxygen results in a partial recovery of the ferroelectric properties. The main goal of the present study is to evaluate the damage induced by FIB etching of PZT films: implantation of Ga³⁺ and film amorphisation. The damaged layer that appears on the films’ surface was thoroughly characterized in terms of the composition and charge implantation but a more detailed characterization seems to be necessary. To address the quality of the nanostructures, the measurement of local electromechanical activity via piezoelectric hysteresis loops acquisition using Piezoelectric response Force Microscopy (PFM) is certainly one of the best options. The conclusion of this work is the development of a suitable process of nano-structures manufacture without introducing piezoelectric property degradation.

2. Description of the structures and experimental set up

2.1 Structure

In this work, we have studied two types of Si/SiO₂/TiO_x/Pt/PZT/Pt structures, namely PZT films being either in amorphous or crystallized state before etching⁹. The films in both

states are deposited by radio frequency magnetron sputtering without substrate heating and therefore the films were amorphous. The film composition is fixed at the morphotropic phase boundary ($Zr/Ti = 54/46$). A post annealing was used to crystallize the PZT film in the Perovskite phase; the annealing temperature was 625°C (conventional annealing) in air during 1/2 hour¹⁰. The film thickness varied between 100 and 300 nm depending on the island diameter, i.e., for a small island diameter the film was thinner to reduce the etching time. Figure 1 presents a typical scheme of the PZT nanostructure (nano island) that we fabricate with the FIB system.

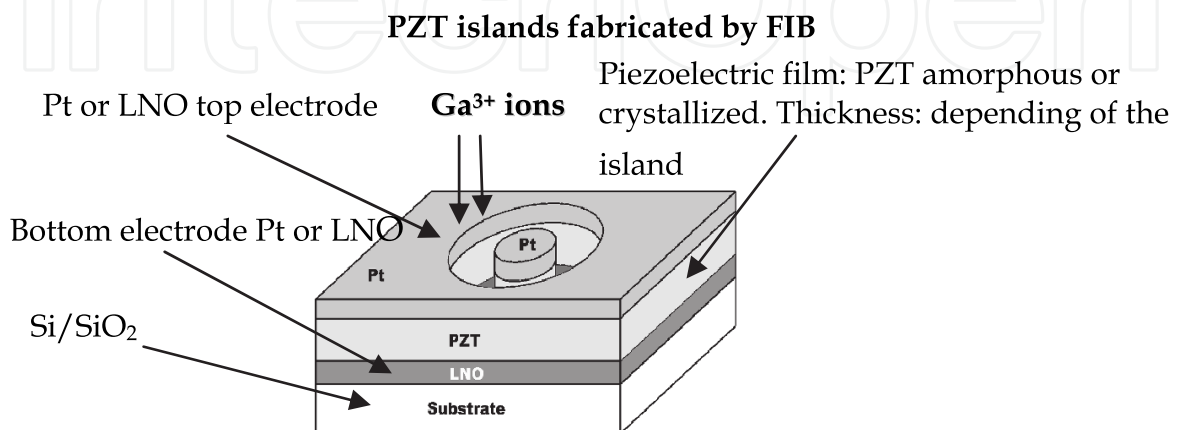


Fig. 1. PZT nano structures (nano island) fabricated by FIB etching on crystallized sample (conventional etching) and on amorphous sample (post annealing after etching).

2.2 FIB system

A focused beam of Ga^{3+} ions (STRATA DB 235 – FEI) was used to pattern the PZT film, Figure 2 shows our FIB system. The system was equipped with both the electron and ion beams.

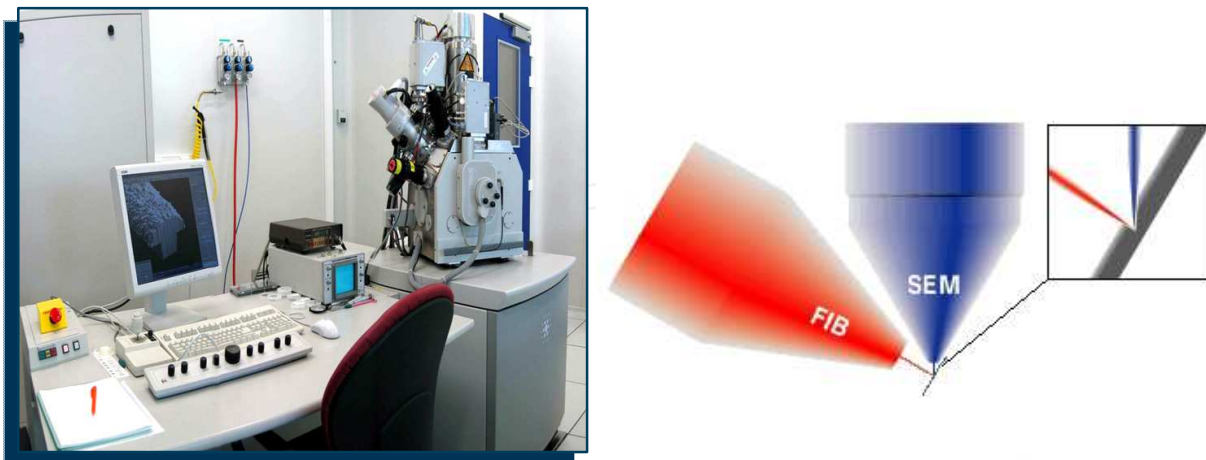


Fig. 2. FIB Machine: FEI dual STRATA 235 – SEM coupling with Ga^{3+} ion beam

The advantage of this system is the possibility to monitor the etching process in real time. The acceleration voltage was 30 kV and ion current was in the range 100 – 10pA depending on the island diameter. We have studied the relation between the current density of the ion beam and its diameter. The ion beam was at the 90° angle to the etched surface.

2.3 Piezoelectric characterization at nano-scale

At nano-scale, the Atomic Force Microscopy (AFM) is currently used¹¹⁻¹⁷. Several AFM techniques, namely, Piezoelectric-response Force Microscopy (PFM) (and its spectroscopic tool which enables the measurement of local piezoelectric hysteresis loops) and Kelvin Force Microscopy (KFM) have been developed and these techniques were used in this work to characterize the piezoelectric nanostructures. For such investigations, a commercial AFM (Multimode, Nanoscope IIIA, Veeco) operating under environmental conditions was used; a scheme of the system is given Figure 3. The local piezoelectric hysteresis loops were obtained by plotting the amplitude of piezoelectric vibration A as a function of the DC voltage in so-called “in-field” mode in order to provide information about electromechanical activity. The frequency and the amplitude of the driving AC voltage were $f = 2$ kHz and $V_{ac} = 1.5$ V, respectively. The applied DC voltage was gradually swept between -10 V and $+10$ V within the period of 200 s. To minimize the electrostatic force effect, Pt/Ir coated Si tips/cantilevers with relatively high spring constant of about 45 N.m⁻¹ were used¹⁶. PFM domain imaging was also performed using the same cantilevers with the spring constant of 3.8 N.m⁻¹ (the frequency and the amplitude of the driving AC voltage were $f = 8$ kHz and $V_{ac} = 1.5$ V, respectively). KFM is a non contact AFM-based technique based on the electrostatic interaction between the tip and the surface. Surface potential maps are easily detected due to work function variation as a result of surface charges, electric dipoles or absorption layer

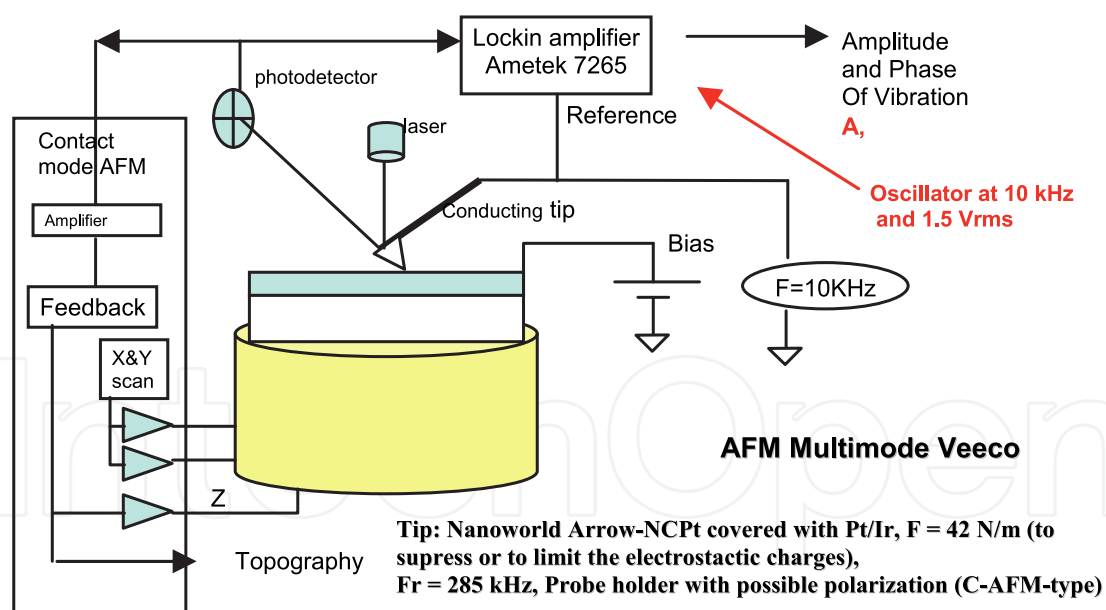


Fig. 3. AFM Multimode Veeco Tip: Nanoworld Arrow-NCPT covered with Pt/Ir, $F = 42$ N/m (to suppress or to limit the electrostatic charges), $F_r = 285$ kHz, Probe holder with possible polarization (C-AFM-type)

2.4 Results and discussion

Before the fabrication of Pt/PZT/Pt islands, we have evaluated the degradation induced by the Ga³⁺ ion beam on the crystallized PZT films deposited on the entire substrate. A large

zone $7 \times 7 \mu\text{m}^2$ was etched at different doses (Figure 4); the Ga^{3+} dose is in relation with number of path of the beam. More precisely, the number of ion beam paths was varied between 1 and 20. According to ¹⁸, the relation between the number of paths and the Ga^{3+} ion dose is the following: ion dose = 4^{13} for 1 path and it become 3^{15} for 20 paths

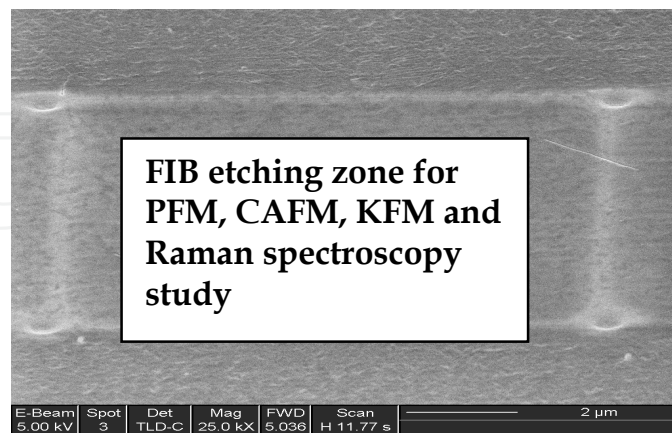


Fig. 4. Scanning Electron Microscopy (SEM) image of an etched zone by Focused Ion Beam (FIB). The dimension of the zone is $7 \mu\text{m} \times 7 \mu\text{m}$. Piezo-response Force Microscopy (PFM) and Kelvin Force Microscopy (KFM) images are made in this zone.

Firstly, we have analyzed macroscopically the defects induced in the material by Raman Spectroscopy. We have compared the responses of different samples: (a) the un-etched crystallized PZT film, (b) after hardest amorphous FIB etching process (Ga ion dose value = 3^{15}), (c) after lightest conventional FIB etching process (dose value = 4^{13}), (d) after hardest conventional FIB etching process (dose value = 3^{15}). The results are presented Figure 5.

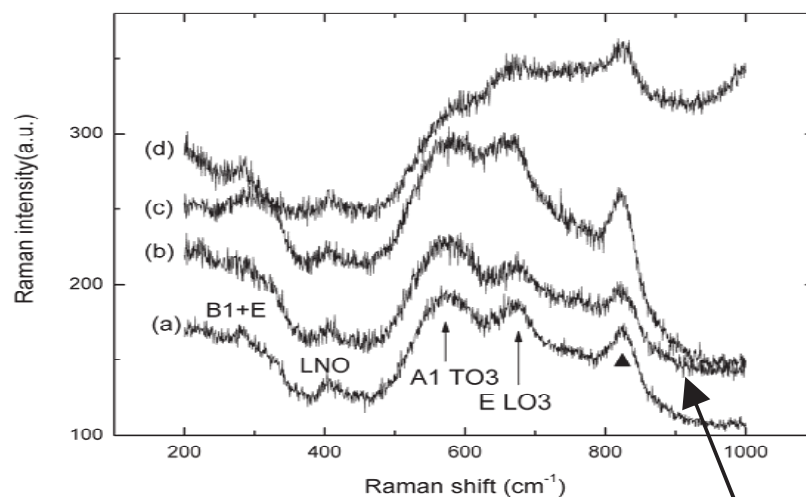
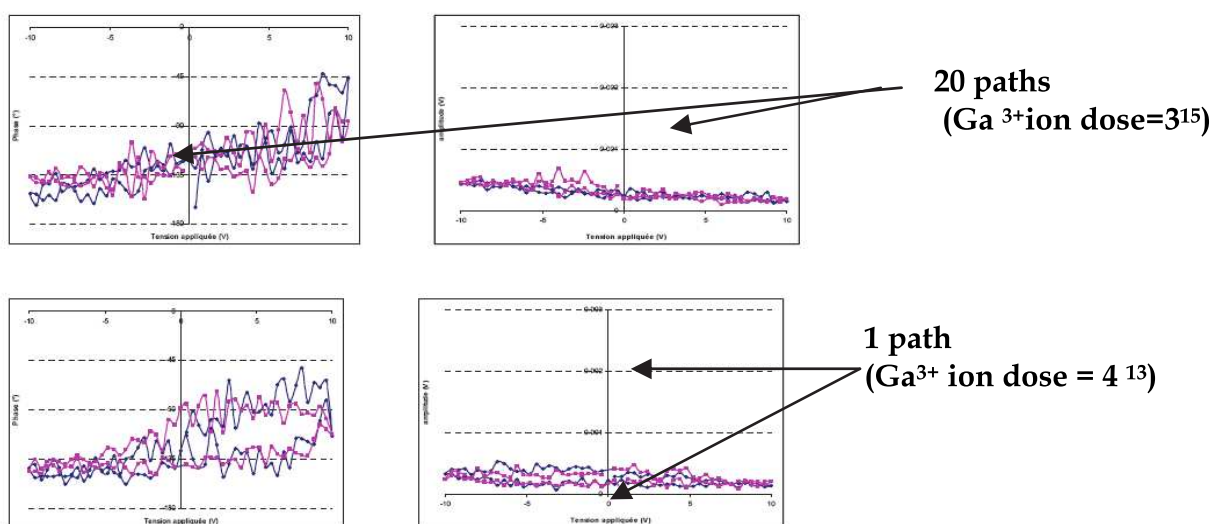


Fig. 5. Raman Spectroscopy on PZT by conventional FIB etching process. The broadband centered at 280 , 572 and 676cm^{-1} → modes in the single PZT crystals

For the hardest conventional etching case, the Raman spectra recorded in the region exposed to the FIB shows an important modification in comparison of single PZT crystals ¹⁹, ²⁰: we observe a sharp increase in the intensity of the Raman peak at 676cm^{-1} which

corresponds to the (E(LO3) mode). This result is certainly connected with the distortion of the tetragonal symmetry of the PZT crystalline lattice due to the ion implantation and the modification of the stress state^{21, 22}. The broadening of Raman scattering in 550-900 cm⁻¹ region could be attributed to the existence of the amorphous material which is usually expected during the conventional FIB etching process.^{23, 24, 25} In conclusion, whatever the FIB etching process, the peak position of Raman shift does not show any change, so the crystalline structure still exhibits perovskite phase.

We have compared the piezoelectric response of three samples (Figure 6): un-etched crystallized PZT film (denoted as sample (a)), amorphous PZT film etched before crystallization (sample (b)) and PZT film etched after crystallization (sample (c)). In crystallized PZT films (sample (c)) we observed strong piezo-response degradation whatever is the ion dose during etching. In fact, no piezoelectric response was obtained even after 1st path. At the same time no ferroelectric domains could be imaged.



❖ Results: PFM measurements of FIB-etched PZT square patterns show that there is no piezoelectric response inside the square. The results suggest that there exist a damaged layer on the surface of the square, which can affect the piezoelectric performance of PZT

Fig. 6. PFM signal (amplitude) on the etched zone (conventional process: PZT crystallized) as a function of the number of paths.

The degradations induce by the FIB are not limited to the etched region; we have observed that even outside the exposed zone, some defects appears. Figure 7 shows this phenomenon, in this example we use the conventional FIB process. The PFM signal is restore at 100 μm outside the etched zone, the explanation can be in relation with the spatial extension of the ions beam. It is well known that the ions beam has a Gaussian form and as a consequence the zone outside the etched region is also in contact with the Ga³⁺ ions beam.

We tried to rejuvenate at least partially, the piezoelectric activity using a post annealing treatment (as it is currently proposed in the literature, e.g. for PZT films etched by RIBE²²), but irrespective of the conditions (temperature, atmosphere) we were unable to restore the initial properties of the films. These results suggest that a damaged layer exists on the surface of the film which affects strongly the piezoelectric performance of PZT

films. These damages could be: amorphisation of film surface, modification of the film composition, etc. In order to understand more the phenomena we analyse the film surface by KFM. The results are presented Figure 8. We show the evolution of the KFM signal as a function of the number of paths, the changing of colour of the etched zone is in relation with the number of paths; when the etched zone is completely degraded, the zone becomes black. Some effects can explain these modifications: lead loss, gallium implantation; some authors have observed the substitution of Ga in the place of Pb to form: GZT (Ga,Zr,Ti) at the film surface.²⁶

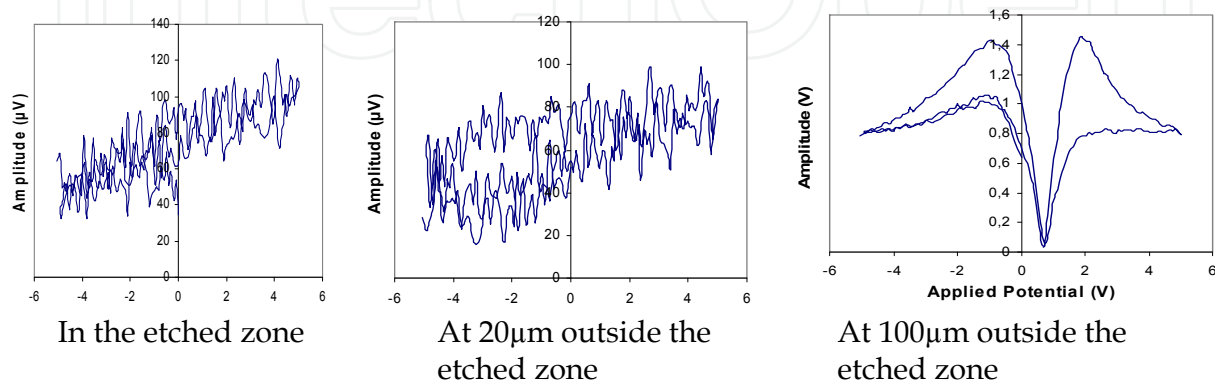


Fig. 7. Extension of the degradations outside the etched zone: influence of the ion beam spatial extension: Gaussian beam.

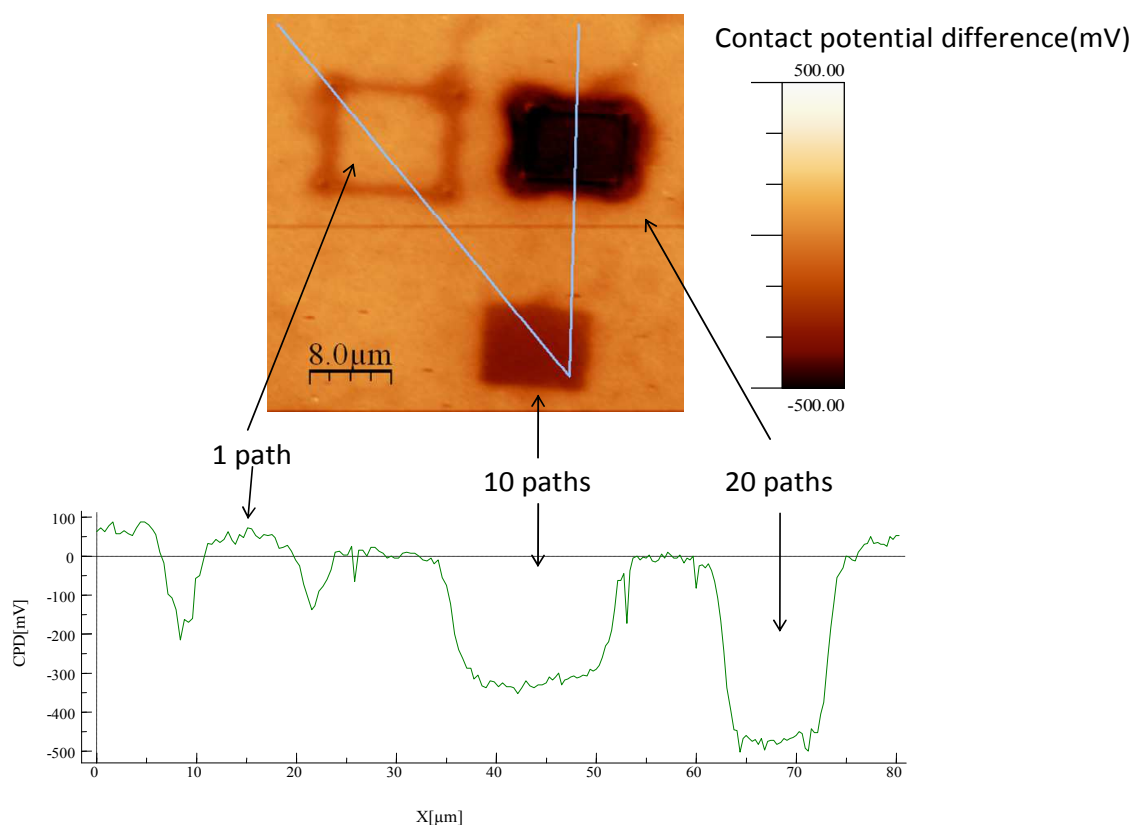


Fig. 8. KFM signal on conventional etching sample measure on areas subjected to different number of paths.

The KFM image of Figure 8 shows the evolution of the tip grounded CPD (Contact Potential Difference) response as a function of the number of paths on the conventional etching sample. The KFM and the CAFM (see later) measurements were made at the same time that means with CAFM configuration the tip is virtually connected to the ground and the bias is applied to the sample. The change of contrast is, of course, directly related to the variation of the surface properties such as the composition and / or amorphisation of the material and induced structural defects. We cannot make more definitive conclusion for the moment but it is clear that after 20 paths the etched region is completely modified. A CPD profile (here the sample is grounded) over the three etched area indicates almost no modification of CPD for 1 path and apparent decrease by 350 mV and 500 mV for 10 and 20 paths, respectively. In our conditions (room and instrument calibration), the CPD of the surface was -50mV relative to a sample grounded. To compare the KFM signals obtained on the samples (b) and (c), we perform a second experiment under the same condition (tip, instrumentation configuration and sample grounding).

The results are presented in Figure 9. The strong contrast difference in the sample (c) (between etched and not-etched areas) confirms the strong damage induced and a consequent modification of the surface potential. On the contrary, only weak damage (small contrast variation) is observed for the sample (b) (etched in the amorphous state). To point out these variations more clearly, we indicate the CPD value across the etched region (Figure 9b).

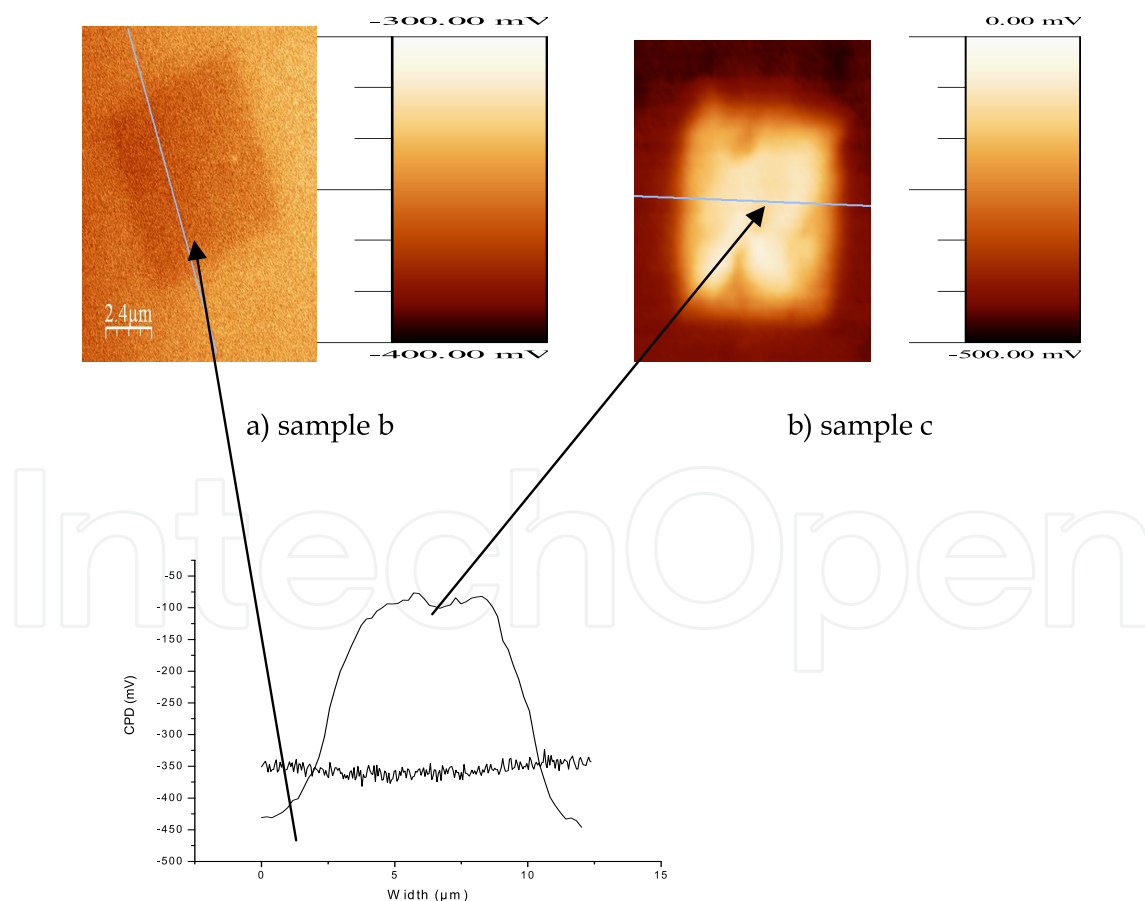


Fig. 9. a) KFM signal measured on amorphous and crystallized film after etching.
b) Cross-section of the contact potential measured sample c. The position of the scan is précised figure a.

It confirms that the potential increase between the un-etched surface and the surface of PZT etched after crystallization is very large (about 300 mV). The implanted charges are the same in both samples but for amorphous sample we can suppose that the annealing treatment induces these charges neutralization and a slight decrease (10 mV) of the CPD is only detected. The properties of the etched area are certainly different depending of the process. The difference, in terms of material is not only due the presence of charge on the sample surface but some crystal defects (dislocations), substitution between Pb and Ga ¹⁷, implantation of metallic Ga³⁺ probably were maintained on sample (c) but not in sample (b) due to the annealing treatment. Figure 4 shows the piezo-response amplitude A measured on etched zone after 1 path and 20 paths in the sample (c) (etched after crystallization). As we can observe, only weak piezoelectric activity is obtained even after one path. The poor ferroelectric properties are confirmed by the absence of the hysteresis on both samples. Therefore, the FIB etching is detrimental to functional properties of PZT. Annealing of these etched zones (in air or in O₂ atmosphere at different temperatures and times) had no effect on piezo-response. On the contrary, for PZT etched before crystallization (sample b), the piezoelectric signal (measured after crystallization) is the same as the one obtained for the sample (a) irrespective of the ion dose. Even if degradation is induced on the sample (b), the annealing treatment (crystallisation of the film) permits to eliminate the damages. These results confirm that the strong degradation occurs on the initially crystallized samples and no degradation happens if the FIB is conducted on amorphous samples.

To conclude this work it is evident that the surface potential is changed after etching, especially for the region exposed to conventional FIB, i.e. on crystallized PZT film. To see it more clearly, we shows the absolute surface potential value across the etching region (Figure 10). It implies that the potential difference between the un-etched surface and the surface after amorphous etching is very small (only about 15mv), while the difference between the un-etched surface and the surface after conventional FIB etching is very large (about 300mv).

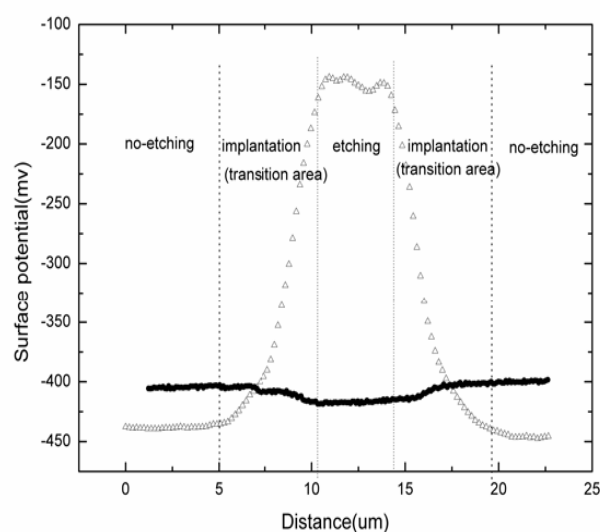


Fig. 10. Absolute film surface potential measured by KFM

So, it is evident that for nanostructures fabrication, the FIB process is very well adapted when the film is in amorphous state (probably due to the lack of grain). So, no degradation

is observed and maybe the post annealing treatment (at temperature equal to the temperature formation of the perovskite phase formation) following the etching process could suppressed the eventual degradations induced is the amorphous one.

In this second part of this work, we focused the results and discussions about the fabrication of PZT nano structures, named nano islands. The typical structures obtained by SEM are shown in Figure 11. The size of the island shown in Figure 11 is 50 nm.

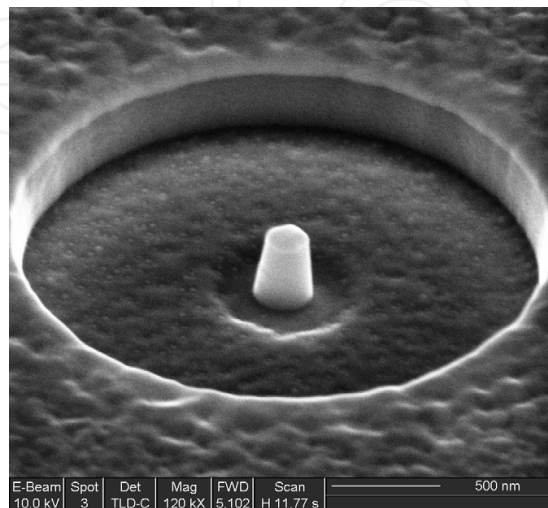


Fig. 11. PZT nano island of 50 nm in diameter

A Pt top electrode was used as a mask to protect the top of the island and, therefore, we take into account only the defects introduced into the islands walls. The etching anisotropy is probably due to the selectivity between Pt and PZT; this effect could be a limitation of the FIB process and it seems more difficult to decrease the island diameter with this technique. The comparative results of the PFM measurements on the PZT islands of 50 nm of size are shown in Figure 12. These results confirm that with conventional etching (on crystallized PZT) the piezoelectric response disappears completely and even after a post annealing treatment the signal could not be restored. On amorphous PZT etching followed by a post annealing treatment at perovskite formation temperature, the piezoelectric response is excellent.

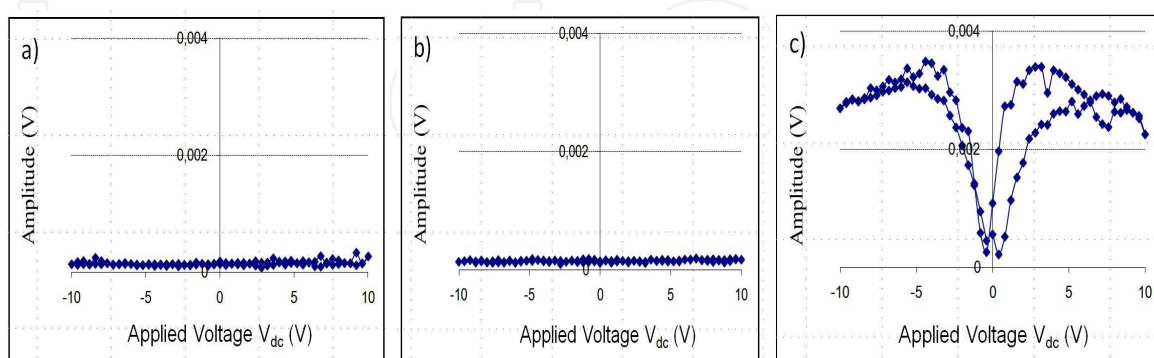


Fig. 12. PFM signal (amplitude) measured on PZT islands of 50 nm after (a) conventional etching process, (b) post-annealing at 625 °C under O₂, (c) amorphous FIB etching process.

These results contradict to those obtained by Stanishevsky *et al.*¹⁷ where the acceleration voltage of the Ga³⁺ ions is larger (50 kV) and so it had to induce stronger degradation. In order to

explain why the piezoelectric signal disappeared we have performed a local I (V) measurements with CAFM on the similar PZT island obtained with the conventional process (etching on crystallized PZT) with 250 nm diameter. The result is shown in Figure 13 for these experiments, a V_{DC} bias was applied to the substrate holder and the top surface Pt was grounded.

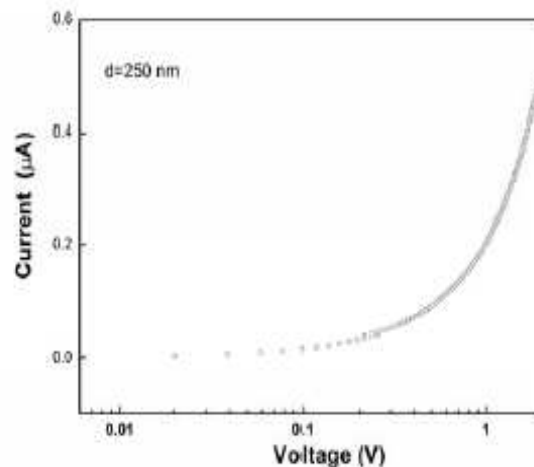


Fig. 13. I(V) measurement on conventional etching sample obtained by Conducting Atomic Force Microscopy (CAFM).

The current increased rapidly with the applied voltage indicating strong local conductivity due to the presence of an electrical conducting channel. This proves a very strong damage due to Ga^{3+} ion implantation in the PZT nano-islands and associated loss of the piezoelectric activity. The leakage current becomes more important when the island diameter decreases, it is thus can be responsible for the results on 50 nm islands. This observed conductivity increase is thus responsible for the weak electromechanical activity observed with the conventional process.

To conclude, we present a new device for BioNEMs applications. It consist of a networks of nano islands (Figure 14) fabricated by FIB. The network is constituted by nano islands of 100 nm; the dimension of the network is $600 \times 600 \text{ nm}^2$

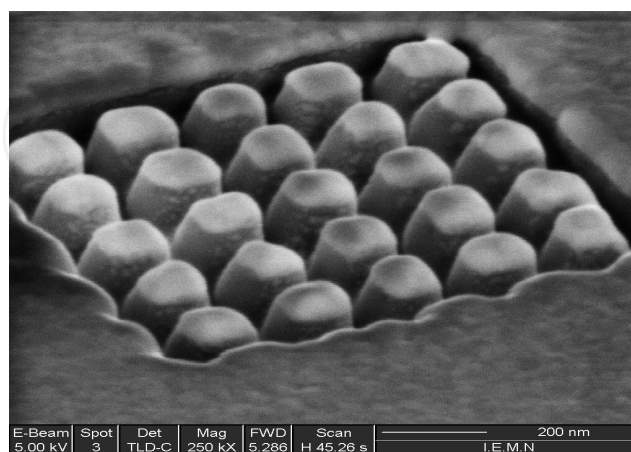


Fig. 14. Network ($600 \times 600 \text{ nm}^2$) of islands (100 nm) for bio application; functionalization of the surface

We measure now the PFM responses of all the nano islands.

3. Conclusion

In conclusion, in this work we have evaluated the damages induced by the Ga³⁺ FIB process for the fabrication of PZT nano structures. Two processes have been developed:

- - the conventional process where the films are crystallized before etching followed by a post annealing to restore the initial piezoelectric electric properties,
- - the amorphous process where the etching process is made on amorphous films followed by a post annealing treatment at the Perovskite formation temperature.

In order to estimate the induced degradations by these two processes we have firstly etched large PZT film zones. The main conclusion is that when the PZT is crystallized in the Perovskite phase a strong degradation is observed and the piezoelectric of the film disappears even after a post annealing treatment. In amorphous state no degradation is observed. So, we have choice this process to fabricate nano piezoelectric structures.

By an optimization of the FIB Ga³⁺ beam and by using amorphous PZT films we have fabricated piezoelectric nano structures: the minimum diameter size of the nano structure is 50 nm. Even at this dimension the nano structure gives always a piezoelectric response. To measure this piezoelectric activity on very small material we have developed and optimized many experimental set up such as : PFM, KFM, CAFM; these methods are relatively news and very well adapted to measurements at nano scale but these methods are very sensitive to external parameters: electrostatic charges, contact between the tip and the material surface,... Many precautions must be taken if you want that these measurements are a true reality of the nano structures performances.

For the nano piezoelectric performances, the conclusions are clear and similar to those obtained on film: with the conventional process, the piezoelectric response disappears (even for large islands (diameter = 800 nm) and even with a post annealing treatment the properties can't be restored. The piezoelectric activity of the nano structure is maintained with the amorphous process. So, the amorphous process is used to fabricate piezoelectric nanostructures. PZT islands of 50 nm in diameter were fabricated and the piezoelectric response was unchanged in comparison with un-etched PZT films. Identical results have been obtained on PMN-PT films. We try in future work to decrease the island diameter and maybe found a diameter where the piezoelectric activity disappears as predicted by some authors (when the dimension of the island = dimension of the domains). A limit exist with the FIB process (due to the anisotropy) and we will try to find this limit and maybe the electron beam lithography will be more adapted for very narrow PZT island (< 50 nm in diameter).

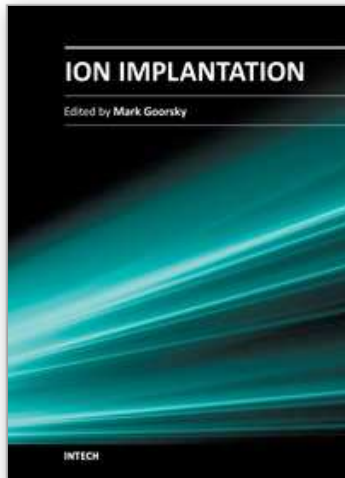
4. Acknowledgement

The authors gratefully acknowledge all the persons who are engaged in this work: Prof. R. Desfeux, and Dr. J.F. Blach from UCCS. Prof. Wang, Prof. Dong and Dr. R.H. Liang from SICCAS - Shanghai.

5. References

- [1] C. Ayela, T. Aleva, D. Lagrange, D. Rémiens, C. Soyer, T. Ondarcuhu, A. Greve, and L. Nicu, IEEE Sensors Journal 8, 210 (2008).

- [2] J. Verd, A. Uranga, G. Abadal, J. Teva, F. Torres, F. Pérez-Murano, J. Fraxeda, J. Esteve, and N. Bardiol, *Appl. Phys. Lett.* 91, 013501 (2007).
- [3] R. R. He, X. L. Feng, M. L. Roukes, and P. D. Yang, *Nano Lett.* 8, 1756 (2008).
- [4] Y. Cho, K. Fujimoto, Y. Hiranaga, Y. Wagatsuma, A. Onoe, K. Terabe, and K. Kitamura, *Nanotechnology* 14, 637 (2003).
- [5] M. Alexe, C. Harnagea, D. Hesse, U. Gösele, *Appl. Phys. Lett.* 75, 1793 (1999).
- [6] C. S. Ganpule, A. Stanshevsky, S. Aggarwal, J. Melngailis, E. Williams, R. Ramesh, V. Joshi, and Carlos Paz de Araujo, *Appl. Phys. Lett.* 75, 3874 (1999).
- [7] R. H. Liang, D. Rémiens, D. Deresmes, C. Soyer, D. Troadec, X.L. Dong, L.H. Yang, R. Desfeux, A. Da Costa, and J.F. Blach, *J. Appl. Phys.* 105, 044101 (2009).
- [8] K. Saito and M. Kaise, *Jpn. J. Appl. Phys.* 31, 3533 (1992).
- [9] M. Detalle, G. Wang, D. Rémiens, P. Ruterana, P. Roussel, and B. Dkhil, *J. Cryst. Growth*, 305, 137 (2007).
- [10] R. Herdier, M. Detalle, D. Jenkins, C. Soyer, and D. Rémiens, *Sensors & Actuators A* 148, 122 (2008).
- [11] S. Hong, J. Woo, H. Shin, J.U. Jeon, Y.E. Park, E. L. Colla, N. Setter, E. Kim, and K. No, *J. Appl. Phys.* 89, 1377 (2001).
- [12] A. L. Kholkin, V. V. Shvartsman, A. Yu. Emelyanov, R. Poyato, M. L. Calzada, L. Pardo, *Appl. Phys. Lett.* 82, 2127 (2003).
- [13] S.V. Kalinin, A. Gruverman and D.A. Bonnel, *Appl. Phys. Lett.* 85, 795 (2004).
- [14] A. L. Kholkin, V. V. Shvartsman, D. A. Kiselev, I.K. Bdikin, *Ferroelectrics* 341, 3 (2006).
- [15] A. Gruverman and S.V. Kalinin, *J. Mater. Sci.* 41, 107 (2006).
- [16] R. Desfeux, C. Legrand, A. Da Costa, D. Chateigner, R. Bouregba, and G. Poullain, *Surf. Sci.* 600, 219 (2006).
- [17] A. Ferri, A. Da Costa, R. Desfeux, M. Detalle, G.S. Wang, and D. Rémiens, *Integr. Ferroelectr.* 91, 80 (2007).
- [18] J. F. Ziegel, *The stopping and Range of Ion in Solid* (Pergamon, New York, 1985).
- [19] J. F. Meng, R. S. Katiyar, and G. T. Zou, *Phys. Status Solidi A* 164, 851, 1997.
- [20] X. Lou, X. Hu, M. Zhang, F. D. Morrison, S. A. T. Redfern, and J. F. Scott, *J. Appl. Phys.* 99, 044101, 2006.
- [21] J. Frantti, V. Lantto, S. Nishio, and M. Kakihana, *Phys. Rev. B* 59, 12, 1999.
- [22] J. F. Meng, R. S. Katiyar, G. T. Zou, and X. H. Wang, *Phys. Status Solidi A* 164, 851, 1997.
- [23] K. Nomura, Y. Takeda, M. Maeda, and N. Shibata, *Jpn. J. Appl. Phys., Part 1* 39, 5247, 2000.
- [24] C. Soyer, E. Cattani, and D. Rémiens, *J. Appl. Phys.* 92, 1048, 2002.
- [25] R. H. Liang, D. Rémiens, C. Soyer, N. Sama, X. L. Dong, and G. S. Wang, *Microelectron. Eng.* 85, 670 _2008_.
- [26] A. Stanishevsky, B. Nagaraj, J. Melngailis, R. Ramesh, L. Khriachtchev, and E. McDaniel, *J. Appl. Phys.* 92, 3275 (2002).



Ion Implantation

Edited by Prof. Mark Goorsky

ISBN 978-953-51-0634-0

Hard cover, 436 pages

Publisher InTech

Published online 30, May, 2012

Published in print edition May, 2012

Ion implantation presents a continuously evolving technology. While the benefits of ion implantation are well recognized for many commercial endeavors, there have been recent developments in this field. Improvements in equipment, understanding of beam-solid interactions, applications to new materials, improved characterization techniques, and more recent developments to use implantation for nanostructure formation point to new directions for ion implantation and are presented in this book.

How to reference

In order to correctly reference this scholarly work, feel free to copy and paste the following:

D. Rémiens, D. Deresmes, D. Troadec and J. Costecalde (2012). Ga³⁺ Focused Ion Beam for Piezo Electric Nano Structuration Fabrication, Ion Implantation, Prof. Mark Goorsky (Ed.), ISBN: 978-953-51-0634-0, InTech, Available from: <http://www.intechopen.com/books/ion-implantation/ga3-focused-ion-beam-for-piezo-electric-nano-structuration-fabrication>

INTECH
open science | open minds

InTech Europe

University Campus STeP Ri
Slavka Krautzeka 83/A
51000 Rijeka, Croatia
Phone: +385 (51) 770 447
Fax: +385 (51) 686 166
www.intechopen.com

InTech China

Unit 405, Office Block, Hotel Equatorial Shanghai
No.65, Yan An Road (West), Shanghai, 200040, China
中国上海市延安西路65号上海国际贵都大饭店办公楼405单元
Phone: +86-21-62489820
Fax: +86-21-62489821

© 2012 The Author(s). Licensee IntechOpen. This is an open access article distributed under the terms of the [Creative Commons Attribution 3.0 License](#), which permits unrestricted use, distribution, and reproduction in any medium, provided the original work is properly cited.

IntechOpen

IntechOpen